RESEARCH PAPER

1-Hexadecylamine as both reducing agent and stabilizer to synthesize Au and Ag nanoparticles and their SERS application

Xiaomiao Hou · Xiaoling Zhang · Yan Fang · Shutang Chen · Na Li · Qi Zhou

Abstract 1-Hexadecylamine (HDA)-capped Au and Ag nanoparticles (NPs) have been successfully prepared by a one-pot solution growth method. The HDA is used as both reducing agent and stabilizer in the synthetic process is favorable for investigating the capping mechanism of Au and Ag NPs' surface. The growth process and characterization of Au and Ag NPs are determined by Ultraviolet–visible (UV–vis) spectroscopy, transmission electron microscopy (TEM), and X-ray diffraction (XRD). Experimental results demonstrate that the HDA-capped Au and Ag NPs are highly crystalline and have good optical properties. Furthermore, surface-enhanced Raman scattering (SERS) spectra of 2-thionaphthol are obtained on the Au and Ag NPs modified glass surface, respectively, indicating that the as-synthesized noble metal NPs have potentially high sensitive optical detection application.

X. Hou · X. Zhang (✉) · S. Chen · N. Li · Q. Zhou
Department of Chemistry, School of Science, Beijing Institute of Technology, Beijing 100081, People's Republic of China
e-mail: zhangxl@bit.edu.cn

Y. Fang (✉)
Beijing Key Lab for Nano-Photonics and Nano-Structure (NPNS), Department of Physics, Capital Normal University, Beijing 100037, People's Republic of China
e-mail: fangyan@mail.cnu.edu.cn

Introduction

Nanoscale noble metal materials have attracted considerable attention because of their unique properties and potential application in catalysis, optoelectronics, biolabelling, spectroscopy etc (Rojluechai et al. 2007; Xia and Halas 2005; Willets and Van Duyne 2007; Merican et al. 2007; Hashmi and Hutchings 2006; Scaffidi et al. 2009; Banholzer et al. 2008). Currently, various synthetic strategies of noble metal nanostructures have been developed in order to get desired properties and functions. Conventionally, Au and Ag NPs are always synthesized by using sodium citrate or sodium borohydride reduction of $HAuCl_4$ and $AgNO_3$ in aqueous solution (Faraday 1857; Lee and Meisel 1982; Fang 1998; Xu et al. 2006). In recent years, the synthesis is also performed in organic solvent using strong or mild reducing agent to reduce different noble metal structures that have good stability and dispersion. Several groups have reported the synthesis of noble metal nanostructures using alkylamine as reducing agent (Ren and Tilley 2007; Shen et al. 2008; Huo et al. 2008; Pastoriza-Santos and Liz-Marzán 2009; Wang et al. 2009; Itoh et al. 2009; Safin et al. 2009). For example, Shen et al. (2008) used oleylamine as reducing agent and surfactant for Au and Ag NPs'

synthesis. Huo et al. (2008) reported ultrathin single crystal Au nanowires with diameter of ∼1.6 nm and length of few micrometers synthesized by simply mixing HAuCl₄ and oleylamine at room temperature. Itoh et al. (2009) formed an oxalate-bridged silver–oleylamine complex with CO_2 evolution to produce Ag NPs with ∼11 nm dimension. Safin et al. (2009) reported the synthesis of HDA-capped Ag NPs through decomposing the complexes formed by complex the derivatives of N-(diisopropylthiophosphoryl)thiourea with silver in hot HDA. Besides, HDA can also be used as solvent, reducing agent, and stabilizing agent to synthesis Ni NPs (Wang et al. 2008). It can clearly be seen that significant efforts have focused on designing new synthetic protocols which demand reducing agents effectively reduce noble metal and provide a robust coating on the noble metal NPs.

Here, we report on HDA as both reducing agent and stabilizer to synthesize Au and Ag NPs. The actual synthetic procedure is unusually simple, and only three chemicals (HAuCl₄/AgNO₃, HDA, and chloroform/toluene) were used throughout the entire synthetic process. Taking advantage of HDA's multifunctional (reducing and capping) capabilities and low price, we demonstrate a much simplified and inexpensive organic phase synthesis approach of noble metal NPs. The Au/Ag NPs modified glass surface serve as active substrates for SERS application. The SERS spectra of 2-thionaphthol molecules are obtained on them. The work offers a general approach to the noble metal NPs that may be important for optical detection application.

Experimental

Materials

HDA and 2-thionaphthol were purchased from Alfa Aesar Chemicals. HAuCl₄·4H₂O, AgNO₃, and solvents were purchased from Beijing Chemical reagents Co. All other reagents were used without further purification.

Synthesis of Au NPs

The Au:HDA molar ratio was varied from 1:30 to 1:80 by keeping Au amount unchanged. An appropriate amount of HDA and HAuCl₄·4H₂O (0.1 mmol)

were dissolved in 6 mL chloroform in a 25-mL three-neck flask. Under nitrogen protection, the mixture was heated to reflux under magnetic stirring. The solution was kept at this temperature for 6 h and cooled down to room temperature. Methanol was added to give a fine deposit of Au NPs. The suspension was centrifuged at 6,000 rpm for 3 min for several times, the supernatant was discarded. The Au NPs were dispersed in 10 mL heptane for further investigation and application.

Synthesis of Ag NPs

3 mmol HDA and 0.2 mmol AgNO₃ were dissolved in 6 mL toluene in a 25-mL three-neck flask. Under nitrogen protection, the mixture was heated to reflux under magnetic stirring. The solution was kept at this temperature for 6 h and cooled down to room temperature. Methanol was added to give a fine deposit of Ag NPs. The suspension was centrifuged at 6,000 rpm for 3 min for several times, the supernatant was discarded. The Ag NPs were dispersed in 10 mL heptane for further investigation and application.

Preparation of samples for SERS measurement

Several drops of heptane dispersion of Au and Ag NPs were dropped onto glass surface, respectively, and dried under ambient condition to form Au and Ag NPs' assemblies. Then, each assembly surface was added one drop of 1×10^{-3} M 2-thionaphthol ethanol solution for SERS measurement.

Instrumentation

The morphologies of Au and Ag NPs were investigated by TEM with an FEI TECNAI F30. Optical absorption spectra were collected at room temperature on a PE Lambda 35 UV–vis spectrometer with 1 cm quartz cuvettes. The structure of the NPs was investigated by XRD using a Rigaku D/MAX 2400 X-ray diffracometer with Cu K_α radiation ($\lambda = 1.5405$ Å). The Fourier transform infrared (FTIR) spectra of the samples were recorded by using a Bruker Equinox 55. The Raman spectrum was recorded by a microprobe Raman system RENI-SHAW 2000, and the excitation line was at 785 nm. The samples were mounted on an XYZ manual stage

of a Leica microscope and the laser beam was focused onto the samples through a 20× objective. The spectra were recorded using a laser power adjusted to about 100 mW and a slit width of 50 μm. The Au and Ag NPs assemblies surface were investigated by scattering electron microscopy (SEM) with a NOVA NanoSEM 430.

Results and discussion

Figure 1 shows the TEM images and XRD patterns of the Au NPs synthesized with different molar ratio of Au:HDA. In our reaction, HDA plays a dual role as effective reducing agents to reduce Au and as stabilizers to provide a robust coating on the Au NPs in a single step. The three representative reactions are performed under the same reaction condition, except that the Au:HDA ratio is changed from 1:30 to 1:80. When the initial Au:HDA ratio is 1:30, the products were a mixture of big NPs (87%)

and small NPs (13%), and the average size of as-synthesized Au NPs is 10.4 ± 1.9 nm as shown in Fig. 1a. When the molar ratio of Au:HDA is 1:50, the average size of Au NPs turned to 9.8 ± 1.8 nm (Fig. 1b), and the size distribution is still large. It seems that the Au salts can be successfully reduced by HDA at this molar ratio (1:50), however, the stabilizer's amount is still insufficient. Thus, more HDA is required in the synthetic process. When the molar ratio of Au:HDA reached 1:80, the size distribution of Au NPs becomes very narrow. As seen in Fig. 1c, the average size of Au NPs is 7.9 ± 0.4 nm. By the comparison of the three TEM images in Fig. 1, it can be seen that an increase in the amount of HDA leads to an obvious size change of the Au NPs from a mixture of big NPs and small NPs (Fig. 1a, b) to uniform NPs (Fig. 1c). Possible reasons for this change are given as follows: the precursor concentration is increased gradually with a decrease of HDA amounts. Under high concentration of precursors, many nuclei form at the beginning of

Fig. 1 TEM images of Au NPs synthesized at different ratios of Au: HDA. **a** Au: HDA = 1:30, **b** Au:HDA = 1:50, **c** Au:HDA = 1:80, and **d** corresponding XRD patterns
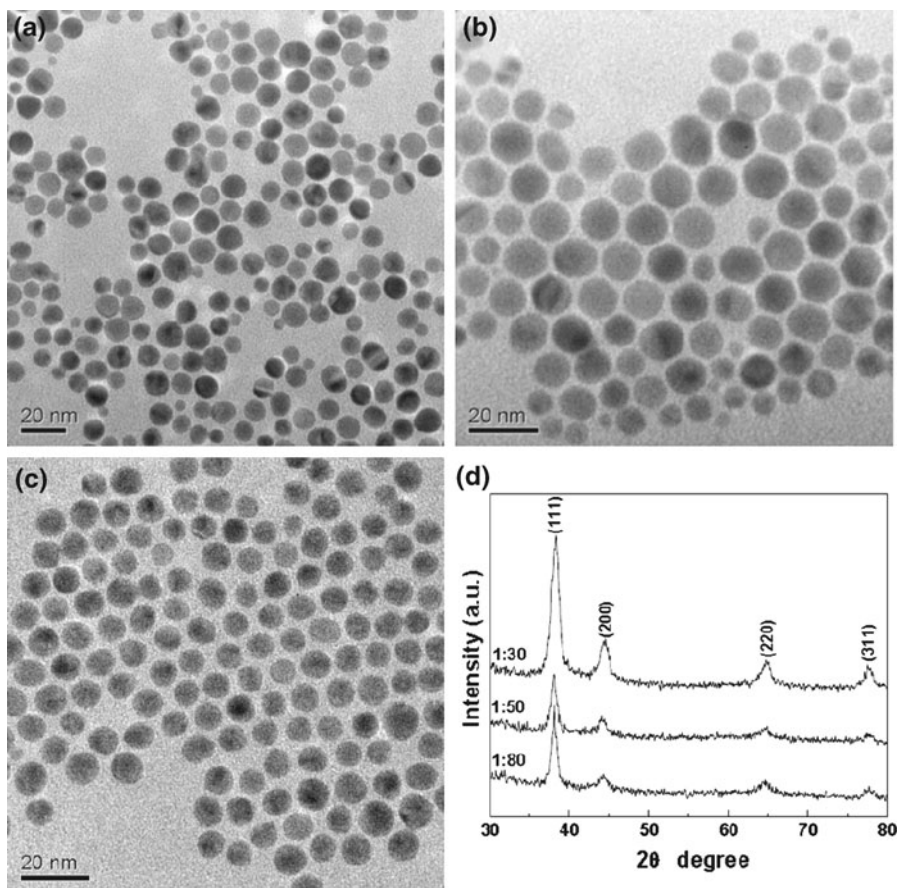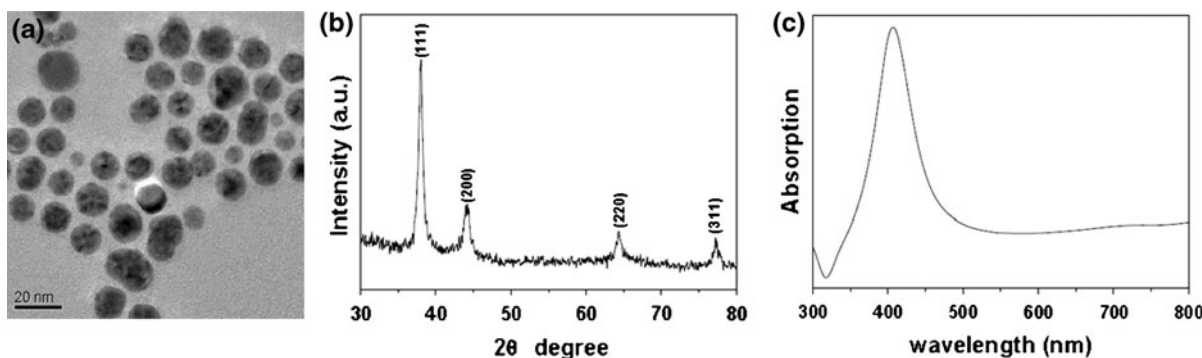
reaction and small quantities of HDA as stabilizer cannot effectively prevent the particles growth, which leads to the formation of mixed Au NPs. An increase of HDA amounts results in an effectively adsorption of the HDA on the NPs' surface, which is of benefit to the synthesis of uniform Au NPs. XRD patterns of the samples obtained at different molar ratio of Au:HDA (Fig. 1d) display the gradual enhancement of the crystallinity of Au products with decreasing of HDA amounts. The diffraction peaks at 38.1°, 44.3°, 64.6°, and 77.5° correspond to (111), (200), (220), and (311) planes of face centered cubic (fcc) Au lattice (JCPDS 89-3697), respectively. The average sizes of Au NPs calculated from (111) reflection by the Scherrer's formula are in agreement with average size obtained from the statistics of the TEM images.
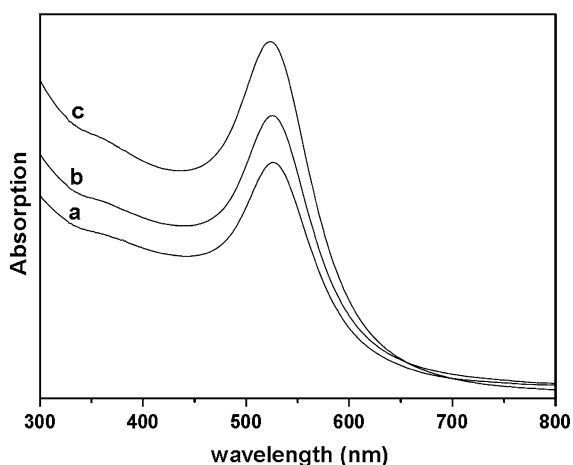
The UV–vis absorption spectra of Au NPs are shown in Fig. 2. With changing of the molar ratio of Au:HDA from 1:30 to 1:80, the absorption bands of as-synthesized Au NPs centered at around 526, 525, and 522 nm, respectively. It is observed from Fig. 2 that the position of the plasmon band is gradually blue shifted from sample a to c. This absorption shift is due to the progressive decrease in the particle size, as larger particles show the plasmon absorbance at longer wavelengths (Jana et al. 2001; Link and El-Sayed 1999). This result is in accordance with the TEM and XRD study. Thus, the size of Au NPs can be adjusted by changing the amount of HDA in the synthetic process.

Using same method, Ag NPs can also be synthesized. As the activity difference between Au and Ag, less HDA is used in the synthetic process. Figure 3a shows the TEM image of Ag NPs synthesized with Ag:HDA of 1:15. It can be seen that the size distribution of HDA-capped Ag NPs is relatively narrow and their average size is 12.3 ± 2.1 nm. The corresponding XRD pattern of the Ag NPs is shown in Fig. 3b. The broadening of the diffraction peaks indicates the small size of the obtained Ag NPs. The diffraction peaks at 38.1°, 44.3°, 64.5°, and 77.4° correspond to (111), (200), (220), and (311) planes of face centered cubic (fcc) Ag lattice (JCPDS 89-3722), respectively. The average size of Ag NPs calculated from (111) reflection by the Scherrer's formula is consistent with the statistic result of the TEM images. The UV–vis absorption spectrum of the as-synthesized Ag NPs is shown in Fig. 3c. The absorption band of Ag NPs centered at around 408 nm, which is similar to other groups' studies (Shen et al. 2008; Wiley et al. 2006). It has been

Fig. 2 UV–Vis spectra of Au NPs dispersed in heptane that synthesized at different ratios of Au:HDA. **a** Au: HDA = 1:30, **b** Au:HDA = 1:50, **c** Au:HDA = 1:80

Fig. 3 TEM image of Ag NPs (**a**), corresponding XRD patterns (**b**) and corresponding UV–vis spectrum (**c**)

documented that sphere Ag NPs exhibit strong surface plasmon resonance (SPR) absorption at around 410 nm (Lu et al. 2009). Thus, monodisperse Ag NPs with good optical properties are also prepared in HDA system by varying the molar ratio of Ag:HDA.

To further confirm the formation of Au and Ag NPs and investigate the interaction between HDA and metal NPs, the FTIR spectra were measured. Figure 4a is the FTIR spectrum of the monodisperse Au NPs that synthesized at the molar ratio of Au:HAD is 1:80. Figure 4b is the FTIR spectrum of Ag NPs that synthesized at the molar ratio of Ag:HDA is 1:15. Figure 4c is the FTIR spectrum of pure HDA. It can be clearly observed from Fig. 4 that the FTIR spectrum of HDA-capped Au and Ag NPs are similar to the spectrum of HDA. In Fig. 4c, the band Vas (–CH$_2$–) at 2,917 cm^{-1}, δas (–CH$_3$) at 1,475 cm^{-1}, and δs (–CH$_3$) at 1,387 cm^{-1}. In Fig. 4a, these bands are also appeared and shifted to 2920, 1460, and 1377 cm^{-1}, respectively. In Fig. 4b, these bands shifted to 2921, 1459, and 1380 cm^{-1}. In Fig. 4a, b, the appearance of these bands indicate that the organic molecules have indeed become a part of the NPs. Besides, the difference in peak intensities of these peaks can also be observed. It is thought that the HDA molecules on the NPs form a relative close-packed HDA layer which constrained the molecular motion, then accounts for the intensity difference between the spectra (Chen et al. 2009; Shen et al. 2003). Furthermore, the band V$_{NH}$ (–NH$_2$) at 3168,

3260, and 3335 cm^{-1}, δ_{NH} (–NH$_2$) at 1,571 cm^{-1} in Fig. 4c cannot be observed in Fig. 4a, b. The amine group has evolved to amide group in Fig 4a, b. Thus, above results indicated that HDA combined with Au and Ag NPs' surface through N atoms.

The as-synthesized Au and Ag NPs have good SERS activity. The Au and Ag NPs modified glass surface were used as substrates for SERS measurement. Figure 5a, b shows the SERS spectra of 2-thionaphthol on Au and Ag NPs modified surface, respectively. Different from the Raman spectrum of 2-thionaphthol solid (Fig. 5c), SERS spectra of 2-thionaphthol in all systems give much more information of vibrational modes for 2-thionaphthol molecules. Not only the number of vibrational modes greatly increased, but also the significant Raman bands split as well as frequencies up and down shift. The detail information of the Raman and SERS modes are laid out in Table 1 (Alvarez-Puebla et al. 2004).

To evaluate the enhancement efficiency of Au/Ag NPs modified substrate, we quote a simple formula to calculate the enhancement factor:

$$G = \frac{I_{SERS}/N_{surf}}{I_{Raman}/N_{bulk}} \quad (1)$$

Here (I_{SERS}/N_{surf}) represents the SERS intensity contributed by 2-thionaphthol molecules in this system and (I_{Raman}/N_{bulk}) represents the normal Raman intensity of species in solution exposed to laser light. Choosing ring stretch mode (around
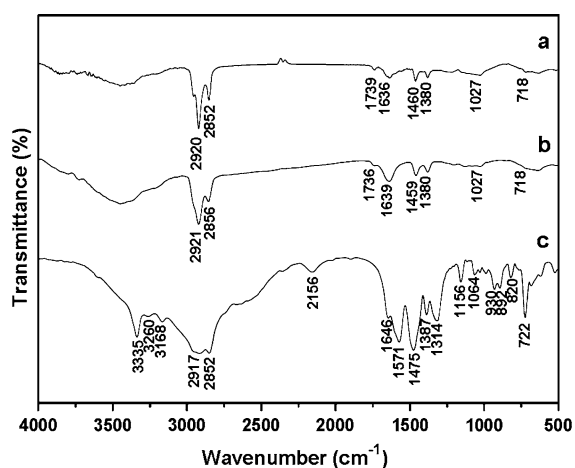

Fig. 4 FTIR spectra of Au NPs modified with HDA (**a**), Ag NPs modified with HDA (**b**) and pure HDA (**c**)
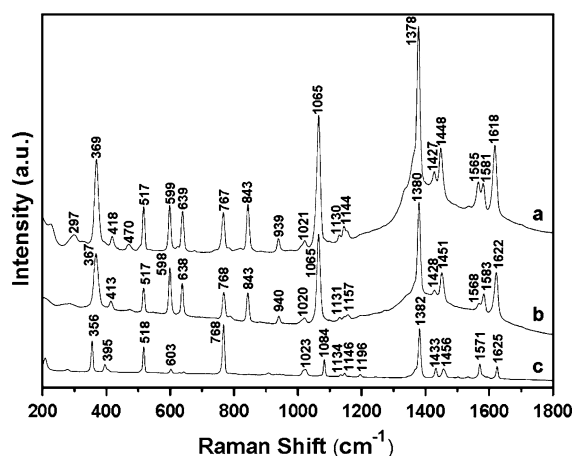
Fig. 5 The SERS spectra of 2-thionaphthol on Au NPs modified glass and (**a**), on Ag NPs modified glass (**b**) and the Raman spectrum of solid 2-thionaphthol (**c**)

Table 1 SERS bands and Raman bands of 2-thionaphthol (cm^{-1})

Raman of solid 2-thionaphthol	SERS of 2-thionaphthol on Au NPs modified glass	SERS of 2-thionaphthol on Ag NPs modified glass	Assignment
	297		Ring wag
356	369	367	Ring deformation and C–S stretch
395	418	413	Ring wag
	470		Ring twist
518	517	517	Ring deformation
603	599	598	Ring deformation
	639	638	Ring twist
768	767	768	C–H wag
	843	843	C–H twist
	939	940	S–H bend
1,023	1,021	1,020	C–H bend
1,084	1,065	1,065	C–H bend
1,134	1,130	1,131	C–H bend
1,146	1,144	1,157	C–H bend
1,196			C–H bend
1,382	1,378	1,380	Ring stretch
1,433	1,427	1,428	Ring stretch
1,456	1,448	1,451	Ring stretch
1,571	1,565	1,568	Ring stretch
	1,581	1,583	Ring stretch
1,625	1,618	1,622	Ring stretch

Fig. 6 SEM images of the surfaces of Au NPs modified glass (**a**) and Ag NPs modified glass (**b**)
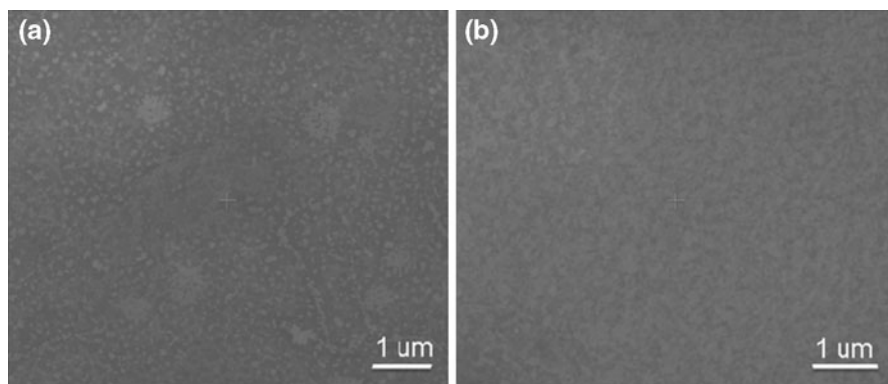
1,380 cm^{-1}) as the typical band, it can be calculated that the enhancement factor G of both Au NPs and Ag NPs modified substrate are about 10^4.

There are two possibilities for molecule adsorption on metal surface, physisorption and the chemisorption. The spectrum of physisorbed molecules is practically the same as the free molecules, differences being observed are only the bandwidths (Weissenbacher et al. 1996). When the molecules are chemisorbed there is an overlapping of the molecular and the metal orbitals, the molecular structure of the adsorbate being modified (Campion and Kambhampati 1998). In our case, it is difficult to separate the contributions of the two mechanisms, which both contribute to the enhancement of the Raman signal. Comparing the SERS spectrum of 2-thionaphthol molecules on Au/Ag NPs modified substrates with the corresponding ordinary Raman spectrum, a shift

of peak positions about 4–20 cm^{-1} can be observed. It indicates that 2-thionaphthol molecules may be chemisorbed on the HDA-capped Au/Ag NPs' surface and the chemical mechanism determined by the charge transfer between molecule and metal may contribute to the giant SERS effects. Besides, there are also exceptions, such as 517, 768, and 1131 cm^{-1} bands, there are nearly no shifts of them, indicating that it is still a physical interaction. Furthermore, the bandwidths in Fig. 5a, b are wider than those in Fig. 5c, indicating that the electromagnetic mechanism contributes to the great enhancement of the Raman signal. Figure 6a, b shows the SEM images of the Au NPs and Ag NPs modified surfaces, respectively. The Au and Ag NPs tend to form uniform structures on glass surface. The close packing of the Au and Ag NPs in a large area assembly can lead to strong interparticle plasmon coupling. Therefore, the SERS signals were enhanced by localized surface plasmon resonance associated with metallic nanostructures.

Conclusions

HDA-capped Au and Ag NPs are synthesized by using a facile one-pot method. In the synthetic process, the HDA serves as both reducing agent and stabilizer, and the particle size is controlled by varying the molar ratio of Au/Ag and HDA. When the molar ratio of Au:HDA is 1:80, the uniform Au NPs can be synthesized effectively. The monodispersed Ag NPs can also be prepared with a method similar to that for Au NPs. These NPs are highly crystalline and show good SERS activity. Therefore, the as-synthesized Au and Ag NPs have the potential to be used in highly sensitive optical detection.

References

Alvarez-Puebla RA, Dos Santos Jr DS, Aroca RF (2004) Surface-enhanced Raman scattering for ultrasensitive chemical analysis of 1 and 2-naphthalenethiols. Analyst 12:1251–1256

Banholzer MJ, Millstone JE, Qin L, Mirkin CA (2008) Rationally designed nanostructures for surface-enhanced Raman spectroscopy. Chem Soc Rev 37:885–897

Campion A, Kambhampati P (1998) Surface-enhanced Raman scattering. Chem Soc Rev 27:241–250

Chen S, Zhang X, Zhao Y, Yan J, Tan W (2009) Preparation and characterization of CdSe nanoparticles in the presence of triocytlphosphine as solvent and capping agent. Mater Lett 63:712–714

Fang Y (1998) Optical absorption of nanoscale colloidal silver: aggregate band and adsorbate-silver surface band. J Chem Phys 108:4315–4318

Faraday M (1857) Experimental relations of gold (and other metals) to light. Philos Trans R Soc Lond 147:145–181

Hashmi ASK, Hutchings GJ (2006) Gold catalysis. Angew Chem Int Ed 45:7896–7936

Huo ZY, Tsung CK, Huang WY, Zhang XF, Yang PD (2008) Sub-two nanometer single crystal Au nanowires. Nano Lett 8:2041–2044

Itoh M, Kakuta T, Nagaoka M, Koyama Y, Sakamoto M, Kawasaki S, Umeda N, Kurihara M (2009) Direct transformation into silver nanoparticles via thermal decomposition of oxalate-bridging silver oleylamine complexes. J Nanosci Nanotechnol 9:6655–6660

Jana NR, Gearheart L, Murphy CJ (2001) Seeding growth for size control of 5–40 nm diameter gold nanoparticles. Langmuir 17:6782–6786

Lee PC, Meisel D (1982) Adsorption and surface-enhanced Raman of dyes on silver and gold sols. J Phys Chem 86:3391–3395

Link S, El-Sayed MA (1999) Size and temperature dependence of the plasmon absorption of colloidal gold nanoparticles. J Phys Chem B 103:4212–4217

Lu X, Rycenga M, Skrabalak SE, Wiley B, Xia Y (2009) Chemical synthesis of novel plasmonic nanoparticles. Annu Rev Phys Chem 60:167–192

Merican Z, Schiller TL, Hawker CJ, Fredericks PM, Blakey I (2007) Self-assembly and encoding of polymer-stabilized gold nanoparticles with surface-enhanced Raman reporter molecules. Langmuir 23:10539–10545

Pastoriza-Santos I, Liz-Marzán LM (2009) N, N-dimethylformamide as a reaction medium for metal nanoparticle synthesis. Adv Funct Mater 19:679–688

Ren JT, Tilley RD (2007) Shape-controlled growth of platinum nanoparticles. Small 3:1508–1512

Rojluechai S, Chavadej S, Schwank JW, Meeyoo V (2007) Catalytic activity of ethylene oxidation over Au, Ag and Au–Ag catalysts: support effect. Catal Commun 8:57–64

Safin DA, Mdluli PS, Revaprasadu N, Ahmad K, Afzaal M, Helliwell M, O'Brien P, Shakirova ER, Babashkina MG, Klein A (2009) Nanoparticles and thin films of silver from complexes of derivatives of N-(Diisopropylthiophosphoryl)thiourea. Chem Mater 21:4233–4240

Scaffidi JP, Gregas MK, Seewaldt V, Vo-Dinh T (2009) SERS-based plasmonic nanobiosensing in single living cells. Anal Bioanal Chem 393:1135–1141

Shen CM, Su YK, Yang HT, Yang TZ, Gao HJ (2003) Synthesis and characterization of n-octadecayl mercaptan-protected palladium nanoparticles. Chem Phys Lett 373:39–45

Shen C, Hui C, Yang T, Xiao C, Tian J, Bao L, Chen S, Ding H, Gao H (2008) Monodisperse noble-metal nanoparticles and their surface enhanced Raman scattering properties. Chem Mater 20:6939–6944

Wang H, Jiao X, Chen D (2008) Monodispersed Nickel nanoparticles with tunable phase and size: synthesis, characterization, and magnetic properties. J Phys Chem C 112:18793–18797

Wang C, Yin H, Chan R, Peng S, Dai S, Sun S (2009) One-pot synthesis of oleylamine coated Au Ag alloy NPs and their catalysis for CO oxidation. Chem Mater 21:433–435

Weissenbacher N, Gobel R, Kellner R (1996) Ag-layers on non-ferrous metals and alloys. A new substrate for surface enhanced Raman scattering (SERS). Vib Spectrosc 12: 189–195

Wiley BJ, Im SH, Li ZY, McLellan J, Siekkinen A, Xia Y (2006) Maneuvering the surface plasmon resonance of silver nanostructures through shape-controlled synthesis. J Phys Chem B 110:15666–15675

Willets KA, Van Duyne RP (2007) Localized surface plasmon resonance spectroscopy and sensing. Annu Rev Phys Chem 58:267–297

Xia Y, Halas NJ (2005) Shape-controlled synthesis and surface plasmonic properties of metallic nanostructures. MRS Bull 30:338–348

Xu ZC, Shen CM, Xiao CW, Yang TZ, Chen ST, Li HL, Gao HJ (2006) Fabrication of gold nanorod self-assemblies from rod and sphere mixtures via shape self-selective behavior. Chem Phys Lett 432:222–225